Characterization of a Solid State DNA Nanopore Sequencer Using Multi-Scale (Nano-to-Device) Modeling

J. Jenkins, D. Sengupta, and S. Sundaram
CFD Research Corporation 215 Wynn Drive
Huntsville, AL 35805
{jwj, dxs, sxs}@cfdrc.com}

ABSTRACT

Nanobiotechnology is a rapidly advancing frontier of science with great potential for beneficial impact on society. Unfortunately, design of integrated nano-bio systems is a complex, laborious task with large failure rates. Current models describing molecular level behavior are expensive, while device design codes lack the necessary nanophysics. The objective of this work is to demonstrate multiscale, multiphysics modeling of an integrated nanobio device, where nanoscale effects are efficiently integrated with a continuum model. A three-level modeling paradigm was developed for this purpose. The feasibility of this approach is demonstrated by characterizing a nanopore-based DNA sequencing device. In the demonstration calculations, the dependence of the device performance on the nucleotide sequence, pore diameter, and applied voltage was determined. Extension of the approach for describing biomolecular processes in other commercial nanobiosystems is discussed. The main conclusions of the device level simulations are presented along with an overview of future work.

***Keywords*:** DNA, nanopore, sequencing, multiscale, modeling.

1 INTRODUCTION

Efforts directed at the problem of integrating nanotechnology and biology to form integrated nano-bio systems are becoming a priority in the research community. Integrated nano-bio systems have emerged as strong candidates for single molecule detection, genomic sequencing, and harnessing naturally occurring biomotors. Understanding the relationship between molecular behavior and system/device response, requires the development of modeling and simulation tools, which can analyze phenomena spanning a wide spectrum of length and time scales. We have developed a hierarchical theoretical and computational framework (Figure 1) that seamlessly couples all levels of computation. Each modeling and simulation level in the hierarchy is chosen with careful attention to a cost-benefit analysis

The first level in the hierarchy is an atomistically detailed model of the nanoscale phenomena of interest. Molecular level simulation enables a physical understanding of the fundamental mechanisms that underlie nanoscale phenomena. The second level of modeling/simulation uses information from the molecular simulations to construct a stochastic model to describe the fast time scale averaged molecular phenomena. The stochastic models are able to reproduce the mean value of interest, along with the fluctuations inherent in the molecular level. The last level of the hierarchy is a continuum model, coupling information taken from the results of the preceding two levels. The stochastic models are tightly coupled to the continuum level for high-fidelity calculations. Insights obtained from the application of such a self-consistent set of tools will have the ability to guide the choice of candidate design strategies for integrated nanobiosystems.

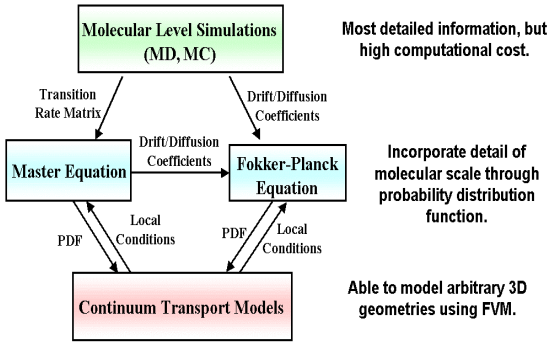

Figure 1: Three level multiscale modeling paradigm.

The example application we have chosen is the problem of DNA translocation through nanpores. This area has come under a great deal of investigation recently due to its promise for inexpensive ultra high-throughput sequencing of DNA. A voltage bias applied to an immobilized α-hemolysin biopore (Figure 2) has been shown to induce charged single stranded DNA and RNA molecules to translocate through the pore. Each translocating molecule blocks the open pore ionic current, providing an electrical signal that depends on several characteristics of the DNA/RNA [1]. The natural pore has limitations due to the fixed size of the pore, thermal stability, and noise characteristics. These difficulties can be circumvented using a suitable solid state nanopore. The demonstration of a voltage biased silicon nanopore detector has been presented in the literature [2].

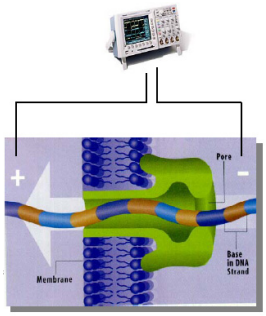

Figure 2: Naturally occurring α-hemolysin biopore [2].

The demonstration calculations presented in this paper are designed to illustrate the coupling of molecular level information into a device level simulation. A description of the molecular modeling is given in §2, followed by the development of the stochastic model in §3. This information is then coupled to the device level calculations to evaluate a proposed ultrahigh throughput DNA sequencing device (§4). The main conclusions of the device level simulations are presented along with an overview of future work.

2 MOLECULAR MODELING

2.1 Construction of the Model

It is known that translocation times can be affected strongly by the pore diameter [1]. Pores with diameters of 1.5nm and 2.0nm, were constructed using the method of Brodka [4]. The SiO_2 slab is truncated to form a solid block of with dimensions of 5nm x 5nm x 5nm [5]. An overhead view of the nanopore is given in Figure 3(a).

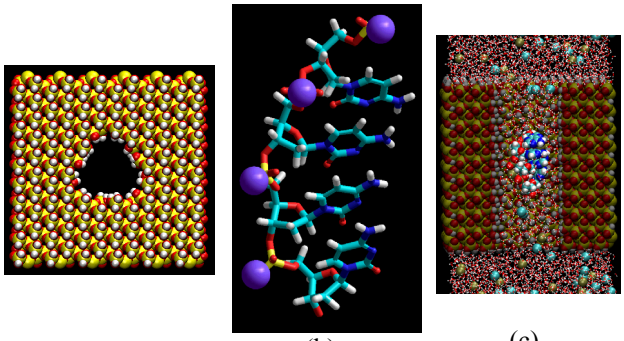

(a) (b) (c)

Figure 3: (a) Overhead view of the 2nm nanopore. (b) 4-mer of Cytosine with potassium counter ions. (c) Cutaway view of final system nucleotide, KCl ions, and water

Experiments have shown that both length and sequence have a significant effect on translocation signal when passing through a nanopore [2]. Two nucleotides were chosen, poly$(dC)_4$ and poly$(dA)_4$, for this computation (Figure 3(b)). The nucleotides were then aligned with the axis of the pore (with the 5' end pointing up) and placed in the nanopore. Water and KCl were added to the system using tcl scripting language built into the VMD molecular graphics software [6]. The final molecular model contains approximately 29,000 atoms.

Molecular Dynamics (MD) simulations were performed (for each case) in three phases following the work of Auffinger [7]. The phases consist of: (a) the initial heating of the water and ions, (b) equilibration of the entire system, and (c) production.

2.2 Translocation Entropy

Entropic effects can contribute significantly to the free energy, especially if a molecule is moving from solution into a confined space. Schlitter's method [8] was used to compute the state entropy from the production phase of the molecular dynamics trajectories.

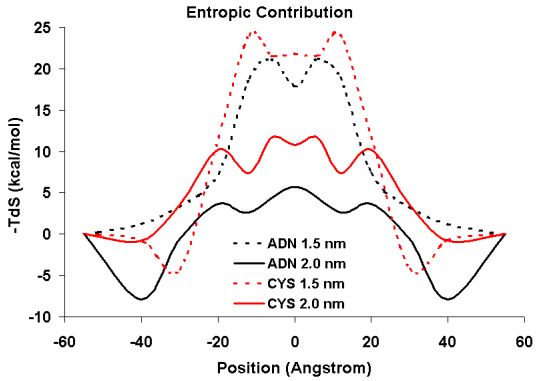

Figure 4: Prediction of the entropic component of the overall free energy of the system

Once the state entropies were computed, the overall free energy contribution (-TΔS) was calculated, and is shown in Figure 4. A striking feature is that the 1.5nm pores have larger entropy changes relative to the surroundings when compared to the 2.0 nm pores. The largest entropic penalty was felt by poly(Cytosine)4 in the 1.5nm pore. This contribution to the free energy is approximately 25 kcal/mol, while the 2nm pore case for cytosine only has a 11 kcal/mol entropic barrier. The adenine shows a similar pattern of higher entropy outside of the pore and higher entropy change for the 1.5nm case relative to the 2.0 nm case.

2.3 Translocation Free Energy

Figure 5 illustrates that the magnitude of the free energy is similar for all four cases. Focusing in on the portion of the graph that contains the pore (–25 to 25 on the x-axis) we can draw some conclusions pertaining to the contribution to translocation times from the free energy.

The relative free energy profiles show that Cytosine has a lower free energy relative to Adenine within the pore, for

both pore diameters, having the lowest free energy in the 1.5nm pore. Adenine shows a lower free energy within the 2.0nm pore relative to the 1.5nm pore, while Cytosine shows a similar free energy for both pores. The barriers extracted from the nanopores are very similar to the shape of the energy profiles extracted from ion channel work [9]. The contribution to the electric field tilts the free energy profiles 11.5 kcal/mol assuming a 120 mV bias across the 5nm thickness of the SiO_2.

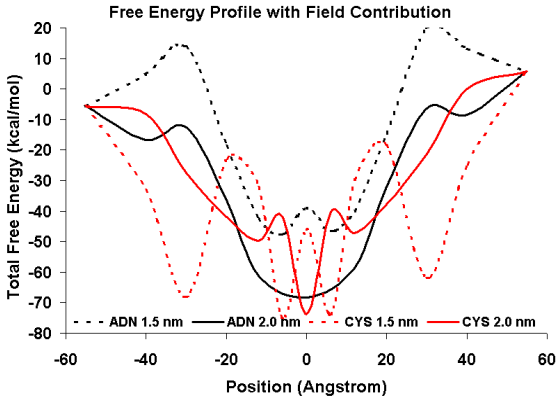

Figure 5: Free Energy Profiles (ΔU-TΔS) of translocation for poly(dC)$_4$ and poly(dA)$_4$ translocating through the 1.5 and 2.0nm pores.

3 STOCHASTIC MODEL

The stochastic model forms the second modeling scale (complementary to the molecular modeling described above). The inputs to this level are the translocation free energy profiles and the dependence of the profile on applied voltage. The general approach of Schulten [10] is followed to compute the mean passage time for a DNA to cross the nanopore, given the free energy profile.

For all four cases, Figure 6 shows an exponential drop in the mean passage time with applied voltage, in agreement with previous work [11]. Looking at the individual nucleotides, the cytosine shows a longer passage time with the 1.5 nm pore as opposed to the 2.0 nm pore. However, the Adenine chain shows a longer passage time with the 2.0 nm pore as opposed to the 1.5 nm pore. Also to note is the fact that there is a much larger difference in passage time comparing pore diameters with cytosine than with adenine. The reason for the differences is clear when we look at the free energy profiles (Figure 5). The Adenine profiles show a large difference in the depth of the minimum on the order of 20% of the total depth. While the cytosine nucleotides do not show the same dependence. The information computed in this section will be coupled in directly with the continuum level model presented in the next section.

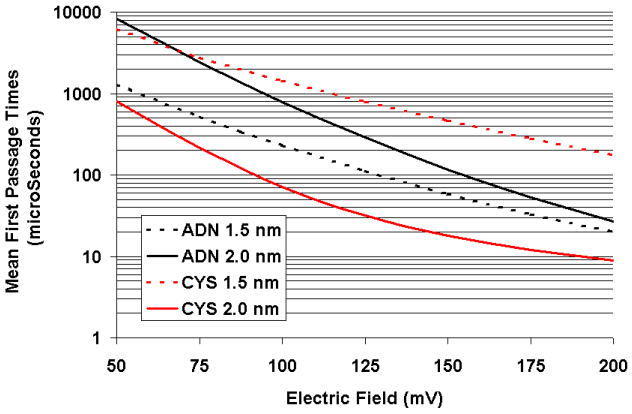

Figure 6: Variation in the mean first passage time with applied electric field for all four cases.

4 CONTINUUM LEVEL MODEL

This forms the final element in the three-tiered paradigm. A pore model is constructed that takes into account the arrival rate of DNA in the proper conformation, and the translocation of DNA across the pore. The method of coupling consists of adding a surface reaction to the continuum model shown in Equation 1.

$$DNA + Pore \xrightarrow{R} Complex$$
$$Complex \xrightarrow{1/\tau} Pore \qquad (1)$$

The surface chemistry contains two steps, with the first step being the rate of capture of a DNA (**R**) chain into the nanopore. This rate was not computed, but was taken from the literature [2]. The second step is to translocate the captured DNA across the pore to free up the pore (Figure 6). This is assumed to occur at a rate of $1/\tau$ where, τ is the mean translocation time computed using the free energy profiles. Both τ and **R** depend upon the applied voltage.

The device chosen for demonstration (Figure 7) is a 21 mm by 7mm by 0.25 mm thick microfluidic chip containing 144 nanopore bearing patches. Within the computational domain of the chip, the Navier-Stokes equation for an incompressible fluid is solved along with the equation of mass transport. At time zero, DNA begins to flow into the chip at a concentration of 10^{-6} Molar and a flowrate of 100 microL/min. The total simulated time is 50 seconds, long enough for the pores to reach a steady state for translocating DNA. Also, a constant voltage was held across each patch, and the magnitude of the electric field was calculated during the simulation. The pore spacing was optimized to minimize electronic cross talk.

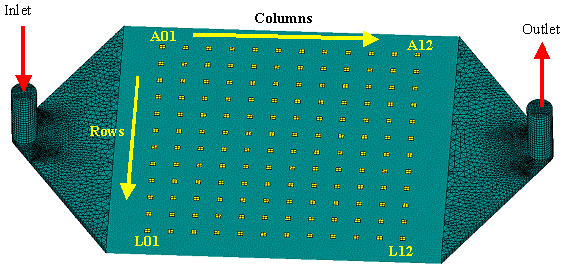

Figure 7: Three dimensional geometry of the notional device showing the labeling of the nanopore containing patches. The patches are shown in yellow.

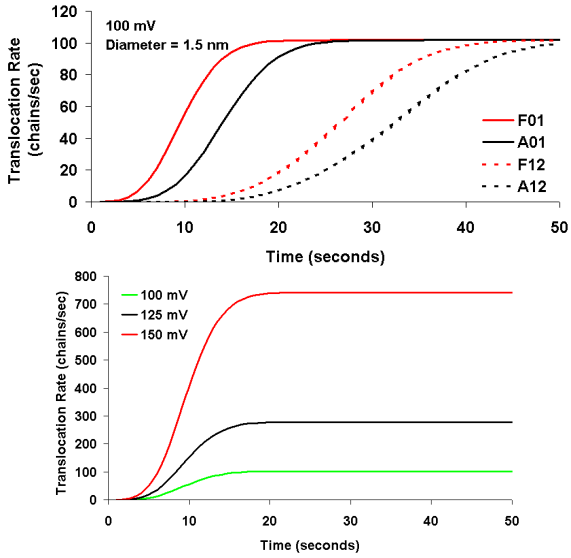

Figure 8: (a) Dependence on the translocation rates on the placement. For the case of CYS 1.5 nm at 100, 125, and 150 mV. (b) Dependence of the translocation signal on voltage and pore diameter.

4.1 Model Dependences

To understand the dependence of the output signals upon pore placement, four pores were monitored: A01, A12, F01, and F12 (see Figure 7 for locations). These represent extremes in terms of placement within the flow field and placement along the line of flow. Figure 8(a) shows the evolution of the translocation rate at the four candidate spots. All three spots show a similar trend of F01 and A01 being the first to reach steady state, while F12 and A12 show a nearly 20 second lag. An increase in the applied voltage increases the point at which the patch translocation rate reaches a steady state. Figure 8(b) shows the dependence of the DNA translocation rates on the applied pore voltage. The translocation rates are shown to increase exponentially in agreement with [11].

5 SUMMARY AND CONCLUSIONS

This paper presents a general three-tiered modeling paradigm for use in simulating devices containing a nanoscale component. The models presented will be incorporated into a continuum code and ultimately used to simulate integrated nanobio devices. Future objectives for this research include the development of a generic framework for simulation of systems of Master Equations and Fokker-Planck Equations. The ME and FPE solver will be designed as a separate module to be integrated with a continuum code for simulations of integrated nano-bio systems. Future work will focus on alternative test systems.

The results from the example calculation show that the overall translocation rate is exponentially dependent on the applied voltage. The placement of the patches of nanopores affects the rate at which they reach a steady translocation rate. The main conclusion from the device level modeling is that in order to improve the performance of this type of a device it is desirable to increase the rate at which DNA is captured. This can be accomplished via the addition of a surface treatment around the pore via functionalization.

6 ACKNOWLEDGMENT

The authors gratefully acknowledge NASA-AMES (NNA04CB26C, Technical Monitor: Dr. Harry Partridge) for funding.

REFERENCES

[1]. Stolc, V., Cozmuta I., Brock, M., O'Keeffe, J., (2003), Presentation given at the DARPA Joint BIOFLIPS/SIMBIOSYS Principal. Investigators Meeting, Monterey, CA.

[2]. Meller, A., Branton D., (2002), Electrophoresis, **23**:2583-2591.

[3]. Li, J., Stein, D., McMullan, C., Branton, D., Aziz, M., and Golovchenko, J., (2001), *Nature* **412**:166-8.

[4]. Brodka, A. and Zerda, T., (1996), *Journal of Chemical Physics* **104**:6319-6326.

[5]. Li, J., Gershow, M., Stein, D., Brandin, E., Golovchenko, J., (2003), *Nature Mat.*, **2**:611-15.

[6]. Humphrey, W., Dalke, A. and Schulten, K., (1996), *Journal of Molec. Graphics*, **14**:33-38.

[7]. Auffinger, P. and Westhof, E., (1997), *Journal of Molecular Biology,* **269**:326-341.

[8]. Schlitter, J., (1993), *Chemical Physics Letters*, **215**:617-21.

[9]. Edwards, S., Corry, B., Kuyucak, S., Chung, S., (2002), *Biophysical Journal*, **83:**1348-60.

[10]. Park, S., Sener, M., Lu, D., Schulten, K. (2003), *J. Chem. Phys.* **119**:1313:19.

[11]. Ambjornsson, T. Apell, S. Konkoli, Z. Marzio, E. Kasianowica, J., (2002), *Journal of Chemical Physics*. **117**:4063-73.